

The puzzling presence of calcite in skeletons of modern solitary corals from the Mediterranean Sea

Stefano Goffredo^{a,*}, Erik Caroselli^a, Francesco Mezzo^a, Leonardo Laiolo^a,
Patrizia Vergni^b, Luca Pasquini^c, Oren Levy^d, Francesco Zaccanti^a,
Aline Tribollet^e, Zvy Dubinsky^c, Giuseppe Falini^b

^a Marine Science Group, Department of Evolutionary and Experimental Biology, Alma Mater Studiorum – University of Bologna, Via F. Selmi 3, I-40126 Bologna, Italy

^b Laboratory of Environmental and Biological Structural Chemistry, Department of Chemistry “G. Ciamician”, Alma Mater Studiorum – University of Bologna, Via Selmi 2, I-40126 Bologna, Italy

^c Department of Physics, Alma Mater Studiorum – University of Bologna, Via Bertini-Pichat 6/2, I-40127 Bologna, Italy

^d The Mina and Everard Goodman Faculty of Life Sciences, Bar-Ilan University, Ramat-Gan 52900, Israel

^e Institut de Recherche pour le Développement, UMR IPSL-LOCEAN, Centre IRD France Nord, 32 Av. Henry Varagnat, 93143 Bondy Cedex, France

Received 26 April 2011; accepted in revised form 10 February 2012; available online 3 March 2012

Abstract

The skeleton of scleractinian corals is commonly believed to be composed entirely of aragonite due to the current Mg/Ca molar ratio of seawater, which thermodynamically favours the deposition of this polymorph of calcium carbonate (CaCO₃). However, some studies have shown that other forms of CaCO₃ such as calcite can be present in significant amount (1–20%) inside tropical coral skeletons, significantly impacting paleo-reconstructions of SST or other environmental parameters based on geochemical proxies. This study aims at investigating for the first time, (1) the skeletal composition of two Mediterranean solitary corals, the azooxanthellate *Leptopsammia pruvoti* and the zooxanthellate *Balanophyllia europaea*, across their life cycle, (2) the distribution of the different CaCO₃ forms inside skeletons, and (3) their implications in paleoclimatology. The origin of the different forms of CaCO₃ observed inside studied coral skeletons and their relationships with the species' habitat and ecological strategies are also discussed. CaCO₃ composition of *L. pruvoti* and *B. europaea* was investigated at six sites located along the Italian coasts. Skeleton composition was studied by means of X-ray powder diffraction and Fourier transform infrared spectroscopy. A significant amount of calcite (1–23%) was found in more than 90% of the studied coral skeletons, in addition to aragonite. This calcite was preferentially located in the basal and intermediate areas than at the oral pole of coral skeletons. Calcite was also mainly located in the epitheca that covered the exposed parts of the coral in its aboral region. Interestingly in *B. europaea*, the calcite content was negatively correlated with skeleton size (age). The presence of calcite in scleractinian corals may result from different mechanisms: (1) corals may biologically precipitate calcite crystals at their early stages in order to insure their settlement on the substrate of fixation, especially in surgy environments; (2) calcite presence may result from skeletons of other calcifying organisms such as crustose coralline algae; and/or (3) calcite may result from the infilling of galleries of boring microorganisms which are known to colonize coral skeletons. We suggest that more than one of the above mentioned processes are involved.

© 2012 Elsevier Ltd. All rights reserved.

* Corresponding author.

E-mail address: stefano.goffredo@marinesciencegroup.org (S. Goffredo).

1. INTRODUCTION

The level of endogenous control of calcium carbonate (CaCO_3) precipitation and a detailed understanding of the biomineralization process of the different forms of CaCO_3 in coral skeletons are major concerns as they can have important implications in interpreting geochemical proxies (Allison et al., 2007; Nothdurft et al., 2007; Dalbeck et al., 2011), and are prerequisites to improve the use of corals as environmental archives (Cuif and Dauphin, 2005). For instance, the presence of only 1% of calcite inside aragonitic coral skeletons can introduce a bias of 1 °C in Sr/Ca based sea surface temperature (SST) paleo-reconstructions (Allison et al., 2007; Dalbeck et al., 2011). The use of coral skeletons as geochemical proxies thus requires a good preservation of trace elements and isotopic ratios which reflect the ambient conditions of seawater in which the skeleton was precipitated. A large variety of endobionts are known to inhabit coral skeletons and early marine cements have been found within corals, thus there is a great need to understand their effects on the geochemistry of coral skeletons (Nothdurft and Webb, 2009b).

Calcite has already been found in significant amount in aragonitic skeletons of some tropical scleractinian corals such as *Porites lobata* (Houck et al., 1975; Nothdurft et al., 2007; Zakaria et al., 2008; Dalbeck et al., 2011), but its origin remains obscure. It was hypothesized that calcite results from microboring fillings (MacIntyre and Towe, 1976; Nothdurft et al., 2007) or diagenesis (Allison et al., 2007). The mechanism involved in precipitation of calcite in microborings remains however unknown. Calcite in coral skeletons could also come from crustose coralline algae, which are often the substrate of fixation for corals in tropical environments (Morse et al., 1988; Heyward and Negri, 1999; Raimondi and Morse, 2000; Baird and Morse, 2004; Harrington et al., 2004; Golbuu and Richmond, 2007) and/or boring bivalves which can be abundant in some coral skeletons (Scott and Risk, 1988; see the review on reef bioerosion by Tribollet and Golubic (2011)). Despite these studies, the abundance, spatial distribution within skeletons and origin of calcite inside corals remain poorly known. Moreover, most studies carried out to investigate the presence of calcite inside coral skeletons concerned reef corals.

In the present study, the skeletal composition of two Mediterranean solitary corals was determined, and when present, calcite was quantified in relation with the size (age) of the studied substrate, its habitat and ecological strategies. One zooxanthellate and one azooxanthellate coral species were selected as model organisms and collected at six different sites along the Italian coasts, to highlight possible difference in the skeletal composition that may be due to the presence of the symbionts or to the different environmental conditions. *Balanophyllia europaea* is a solitary, ahermatypic, zooxanthellate, scleractinian coral, endemic to the Mediterranean Sea (Zibrowius, 1980), with a distribution restricted to 0–50 m depth (Zibrowius, 1980). Its population density can reach dozens of individuals per square meter (Goffredo et al., 2004a). Due to the negative effects of increasing temperature on its growth and popula-

tion dynamics parameters, there is concern for its future in the context of global change (Goffredo et al., 2008, 2009a). *Leptopsammia pruvoti* is an ahermatypic, azooxanthellate, solitary scleractinian coral, which is widely distributed in the Mediterranean basin and along the European Atlantic coast from Portugal to Southern England. It is one of the most common organisms under overhangs, in caverns, and crevices at 0–70 m depth, reaching up to thousands of individuals per square meter (Zibrowius, 1980; Goffredo et al., 2007). The yellow color and high density of polyps make this species attractive for recreational divers, who represent an important income for coastal tourist resorts in the Mediterranean (Mundet and Ribera, 2001).

The aims of this study are: (1) to determine the skeletal composition of the two coral species, (2) to locate and to quantify calcite if present in their skeletons, and (3) to compare for the first time their mineralogy in relation with their size (age), habitat and ecological strategies (symbiotic or non-symbiotic). The origin of calcite in studied coral skeletons is then discussed. This is the first detailed study of presence and abundance of calcite in coral skeletons, at different levels, and the first study of skeleton composition of Mediterranean solitary corals.

2. MATERIALS AND METHODS

2.1. Sampling

From 9 November 2003 to 27 July 2008, specimens of *B. europaea* (Risso 1826) and *L. pruvoti* Lacaze-Duthiers, 1897



Fig. 1. Map of the Italian coastline indicating sites where corals were collected. Abbreviations and coordinates of the sites in decreasing order of latitude: GN, Genova, 44°20'N, 9°08'E; CL, Calafuria, 43°27'N, 10°21'E; LB, Elba Isle, 42°45'N, 10°24'E; PL, Palinuro, 40°02'N, 15°16'E; SC, Scilla, 38°01'N, 15°38'E; PN, Pantelleria Isle, 36°45'N, 11°57'E.

were randomly collected in each of the six study sites located along the Italian coasts (Fig. 1). Different locations were selected to check for general trends related to the latitudinal variations of solar radiation and SST (see Goffredo et al. (2007)). Corals were collected by SCUBA divers at the depth of 5–7 m depth on reefs facing south for *B. europaea*, and at 15–17 m under natural overhangs and caves for *L. pruvoti*. The sampling was performed at depths known to have high population densities and where previous studies on the reproductive biology, biometry, growth and population dynamics and genetics of the two species have been performed (Goffredo et al., 2002, 2004a,b, 2006, 2007, 2008, 2009a,b).

2.2. Preparation of coral skeletons

Collected corals (between 49 and 135 polyps per site for *B. europaea* and between 76 and 210 for *L. pruvoti*, depending on the site) were treated with a solution of 0.05% sodium hypochlorite to remove live tissue without dissolving the skeleton (Pingitore et al., 1993). The remaining skeletons were then washed with distilled water and dried at 50 °C for 4 days (Goffredo et al., 2007, 2008, 2009a). A low drying temperature was chosen to avoid phase transitions in the skeletal aragonite/calcite composition (Vongsavat et al., 2006). Each skeleton was accurately observed under a binocular microscope to remove fragments of rock and calcareous deposits produced by other organisms, such as serpulid tubes and bryozoan colonies (Goffredo et al., 2007, 2008, 2009a). For each skeleton, the length (L , major axis of the oral disc), width (W , minor axis of the oral disc) and height (h , oro-aboral axis) were measured with calipers and dry skeletal mass (M) was measured with a precision balance (Chadwick-Fuman et al., 2000; Goffredo and Chadwick-Furman, 2003; Goffredo et al., 2002, 2004a, 2006, 2007, 2008, 2009a). The age of each skeleton of *B. europaea* was obtained by applying the age-size relationships previously obtained at the same sites and depths (Goffredo et al., 2004a, 2008). Age of *L. pruvoti* skeletons was not determined as the age-size relationship is currently under study. Three different preparations of skeletons were then performed to study (1) the whole skeletal composition, (2) the different regions of skeletons, i.e. aboral, intermediate and oral regions, and (3) the external layer of coral skeletons.

2.2.1. Preparation for analyses of whole coral skeleton composition

At each site, a subsample of 15–21 whole skeletons of *B. europaea* depending on the site, and 14 skeletons of *L. pruvoti* were randomly chosen to analyze the mineral phase content. Then, each skeleton was ground in an agate mortar to obtain a fine and homogeneous powder before further analyses. The grinding time was no longer than 5 min. To reveal the presence of grinding effects, or artefacts, on the mineral phase composition, some samples were ground for longer periods of time, up to 2 h. Also the cleaning effect was tested putting some ground samples for 12 h in a sodium hypochlorite solution (3%) to verify that no dissolution of calcium carbonate skeletons occurred.

2.2.2. Preparation for analyses of specific skeletal section composition

Another subsample of three skeletons per site for each coral species was randomly chosen to analyze the mineral phase content in three different areas of coral skeletons: the aboral section (at the base of the skeleton), the oral section (at the apex of the skeleton), and the intermediate section (between the other two; Fig. 2). Each skeleton was cut at 3 mm from the base (thus obtaining the aboral section) and at 7.5 mm from the base (thus obtaining the intermediate and oral sections; Fig. 2) using a diamond saw mounted on an electric drill (DREMEL® 300 Series). Each section was then ground in an agate mortar to obtain a fine and homogeneous powder before further analyses. For each section of *B. europaea*, the average age of the coral at the time of deposition of the section was estimated by calculating the amount of material produced in each year of growth in each section, using the previously obtained growth models for each population (Goffredo et al., 2004a, 2008).

2.2.3. Preparation for analyses of composition of skeleton external layer

Powder samples were also collected from the most external layer of the skeleton of both species by scratching with a scalpel three skeletal regions: (1) the basal plate, (2) the aboral region, which usually consists of an epitheca-like structure (which we will term epitheca throughout this study; see Nothdurft and Webb, 2009a), and (3) the oral region of skeleton wall. The external layer of the basal plate and of the epitheca was easily detectable and covered the coralline septa (Fig. 3). The mineral phase of these samples was then analyzed (see Section 2.4).

2.3. X-ray powder diffraction analyses

The 103 whole skeleton powders of *B. europaea* (Section 2.2.1), the 84 whole skeleton powders of *L. pruvoti* (Section

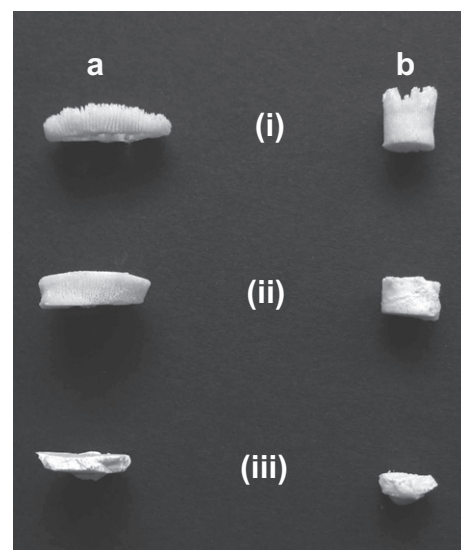


Fig. 2. *Balanophyllia europaea* (a) and *Leptopsammia pruvoti* (b). Oral (i), intermediate (ii), and aboral (iii) sections of the skeletons.

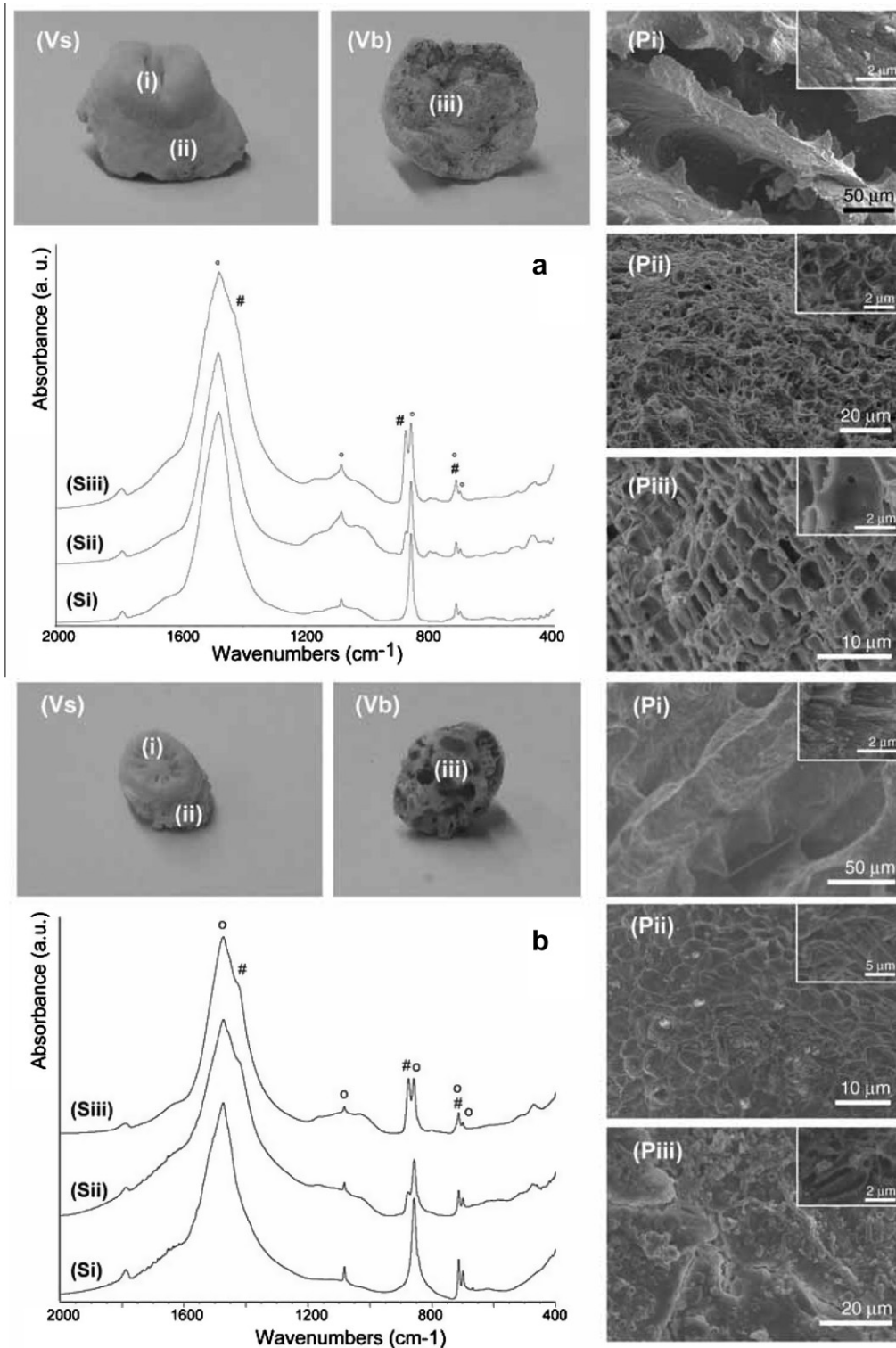


Fig. 3. *Balanophyllia europaea* (a) and *Leptopsammia pruvoti* (b). Structural and morphological characterization of calcium carbonate in the skeleton. (Vs) and (Vb) show a side and basal plate view of a skeleton, respectively. The three regions corresponding to the oral region of skeleton wall (i), the epitheca (ii), and the basal plate (iii) are indicated. The pictures (Pi), (Pii) and (Piii) are scanning electron microscope images corresponding to the regions (i), (ii), and (iii), respectively. In each of these pictures the inset shows a corresponding magnified image. The FTIR spectra of the material scratched from these regions are shown in (Si), (Sii), and (Siii) respectively. The main absorption bands of aragonite (°) and calcite (#) are indicated.

2.2.1), the 54 sections powders of *B. europaea* (Section 2.2.2) and the 54 section powders of *L. pruvoti* (Section 2.2.2) were analyzed by means of X-ray powder diffraction (XRD) using an X-Celerator powder diffractometer (PANalytical) for a qualitative and quantitative analysis of calcium carbonate polymorphism. A diffractogram was obtained for each sample using the following settings: tension = 40 kV; current 40 mA; Cu k-alpha radiation ($\lambda = 1.540 \text{ \AA}$); entry slit $1/2^\circ$; exit slit $1/2^\circ$; step time 60 s; step size 0.02° ; initial $2\theta = 20^\circ$; final $2\theta = 60^\circ$ (Fig. 4). These parameters were optimized for the samples after preliminary trials. For three random skeleton powders per site and three random section powders per site the analysis was repeated to check measurement reproducibility. Identical X-ray powder diffraction patterns were collected. A quantitative analysis of the crystalline phases was performed using the software “Quanto” (see www.ic.cnr.it/Varie/quantohelp/help/geninfo.htm), which is based on the Rietveld method (Altomare et al., 2001; Marchegiani et al., 2009). The agreement index GoF was used as a figure of merit of the refinement process. It is defined as follows:

$$\text{GoF} = R_{\text{wp}} / (N_p - P),$$

$$R_{\text{wp}} = \left\{ \sum w_i [Y_o(i) - Y_c(i)]^2 / \sum w_i Y_o(i)^2 \right\}^{1/2},$$

where $Y_o(i)$ is the measured count at the step i , $Y_c(i)$ is the calculated count at the step i , $w_i = 1/Y_o(i)$, N_p is the total number of counts and P is the number of refined parameters (Altomare et al., 2001). GoF ranged between the best value of 2.21 and the worst one of 5.15. The latter were associated with the lowest content of calcite in the

calcite–aragonite mixtures. To test the validity of the method we prepared mixtures with known calcite–aragonite ratio in the range 0–3% (w/w) using sea urchin spine and nacre as source of pure calcite and pure aragonite, respectively. The Rietveld quantitative analysis of these samples was in good agreement with the experimental data, the difference between calculated and experimental content of calcite being never higher than 0.3% (see [Electronic annex EA-1](#)). The isomorphous substitution of magnesium ions to calcium ions in the calcite structure was estimated by the analysis of the unit cell parameters of calcite. These were refined during the quantitative analysis of the mineral phase and checked also by the position of the calcite diffraction peak corresponding to the planes {104} (Goldsmith et al., 1961; Falini et al., 1994).

2.4. Fourier transform infrared spectroscopy analyses

Low amount powder samples of external layers (basal plate, epitheca, oral skeletal wall; Section 2.2.3) were analyzed by means of Fourier transform infrared spectroscopy (FTIR), using a Nicolet FTIR 380 spectrometer working in the range of wavenumbers $4000\text{--}400 \text{ cm}^{-1}$ at a resolution of 4 cm^{-1} . This technique allows studying small amounts of material otherwise not analyzable using XRD. FTIR allows a qualitative and quantitative analysis of calcium carbonate polymorphism, however we observed that the detection limits of calcite using FTIR (3%) is higher than using XRD (0.5%), for this reason we carried out the quantitative analysis by XRD. Disks were obtained by mixing 1 mg of powdered sample with 200 mg of potassium bromide (KBr,

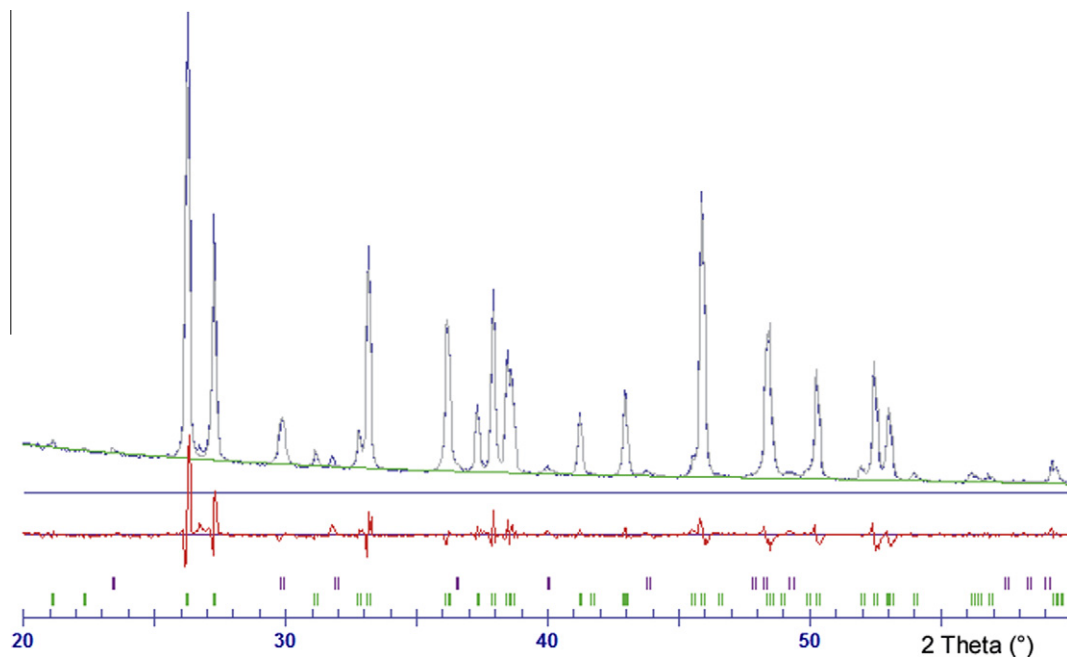


Fig. 4. *Balanophyllia europaea*. X-ray diffraction pattern of the material from a whole skeleton containing 94.2% (SE = 0.2%) of aragonite and 5.8% (SE = 0.2%) of calcite. The diffraction peaks associated to calcite and aragonite are shown by green and purple lines, respectively. The red pattern indicates the difference between experimental and calculated patterns, as obtained applying the Rietveld software for quantitative analyses “Quanto” (www.ic.cnr.it/Varie/quantohelp/help/geninfo.htm; Altomare et al., 2001). (For interpretation of the references to colour in this figure legend, the reader is referred to the web version of this article.)

Sigma Aldrich, FTIR grade, $\geq 99\%$) and applying a pressure of 10 t to the mixture. Obtained qualitative data were analyzed with the software EZ OMNIC (Thermo Electron Corporation). This technique was also used on random samples of Sections 2.2.1 and 2.2.2 (30% of whole dataset) to confirm the X-ray powder diffraction data.

2.5. Morphological and elemental analyses of skeletal samples

Sample morphology, presence/absence of microborings and elemental analysis were performed on one skeleton of *B. europaea* and one skeleton of *L. pruvoti* per study site (total $N = 12$) using a scanning electron microscope (SEM; Philips XL 20) equipped with an EDX detector (Philips Xd-4). The observations were carried out using a tension of 20 kV. Samples were glued on an aluminium stub and coated by sputtering with a gold or carbon layer prior the observation.

2.6. Statistical analyses

The data sets did not present a normal distribution nor homoscedasticity, thus non parametric tests were performed (Potvin and Roff, 1993). Kruskal–Wallis test was used to compare mean skeletal length, age and calcite content per coral species among sites, and mean calcite content between aboral and oral sections within each coral population. Tukey's honestly significant difference (HSD) was used to indicate which means of calcite content in *L. pruvoti* populations were significantly different from each other (Tukey, 1949). All the analyses were performed with the software SPSS 12.0.

3. RESULTS

3.1. Whole skeleton composition

Calcite was found in addition to aragonite in more than 92% of the skeletons of *B. europaea* and *L. pruvoti* (93.2%

and 92.9%, respectively). In the remaining samples calcite content was not detectable by X-ray diffraction. The presence of calcite in the skeleton could not be ascribed to a phase transition which occurred during the grinding process or to a dissolution re-precipitation process during the tissue cleaning stage. This is because samples of skeleton containing only aragonite did not show any detectable trace of calcite after two hours of grinding for *B. europaea* and one hour of grinding for *L. pruvoti*. The usual grinding time was shorter than 5 min. Also, a long treatment of the powdered skeletons in a sodium hypochlorite solution did not cause any transition from aragonite to calcite.

In *B. europaea*, calcite weigh represented 1–23% of the total skeleton mass. Samples of *L. pruvoti* contained 1–21% of calcite. No other mineral phases (e.g. calcium phosphates) were detected by XRD or FTIR techniques. The calcitic phase observed in skeletons always showed a reduction of the lattice parameters, ascribable to the isomorphic substitution of magnesium ions to calcium ions. The average magnesium to calcium molar percentage of isomorphic substitution in the calcite structure ranged from 8.9% to 14.5% and from 8.5% to 12.1% in *B. europaea* and *L. pruvoti* skeletons, respectively (Table 1). No significant correlation was observed among magnesium content in the calcite structure and sample collection site ($P > 0.05$; Table 1).

In *B. europaea*, mean length, age and calcite content of analyzed skeletons did not vary significantly among sites (Kruskal–Wallis test, $P > 0.05$; Table 1). For each studied site, calcite content was negatively correlated with both skeleton length and age (Fig. 5). Skeleton length explained 25.1–71.5% of calcite content variance and skeleton age explained 25.5–76.4% of variance (Fig. 5).

In *L. pruvoti*, mean length (age) of analyzed skeletons did not vary significantly among sites (Kruskal–Wallis test, $P > 0.05$; Table 1), while mean calcite content varied significantly among sites (Kruskal–Wallis test, $P < 0.05$; Table 1). Two clusters of homogeneous populations were found for *L. pruvoti*: one characterized by high calcite content (Calafuria; mean calcite content = 5.8%) and another which contained less calcite (all the other sites; mean calcite

Table 1
Balanophyllia europaea and *Leptopsammia pruvoti*. Mean length, calcite content, and Mg to Ca substitution in the calcite content of whole skeletons in the populations. Values in parentheses are the 95% confidence intervals. N , number of individuals.

Population	Code	N	Mean length (mm)	Mean age (years)	Mean % calcite	Mean % Mg in calcite
<i>Balanophyllia europaea</i>						
Genova	GN	15	12.3 (9.0–15.5)	9.2 (5.7–12.8)	2.2 (1.2–3.3)	11.9 (9.7–14.0)
Calafuria	CL	17	10.0 (8.0–12.0)	6.3 (4.5–8.2)	2.3 (1.2–3.3)	8.9 (7.0–10.8)
Elba	LB	15	11.8 (9.2–14.5)	9.0 (5.7–12.4)	3.9 (1.9–5.9)	14.5 (13.9–15.2)
Palinuro	PL	18	11.3 (9.3–13.3)	9.8 (7.5–12.1)	3.7 (1.1–6.3)	11.9 (9.8–13.9)
Scilla	SC	21	9.6 (8.0–11.2)	7.0 (5.6–8.5)	2.9 (1.9–3.9)	10.5 (8.8–12.2)
Pantelleria	PN	17	11.2 (8.8–13.7)	9.2 (6.8–11.5)	2.3 (1.5–3.2)	10.1 (8.3–11.9)
<i>Leptopsammia pruvoti</i>						
Genova	GN	14	5.7 (4.4–6.9)	–	1.7 (0.9–2.5)	10.2 (8.3–12.2)
Calafuria	CL	14	4.6 (3.6–5.6)	–	5.8 (2.5–9.0)	10.8 (9.2–12.4)
Elba	LB	14	6.0 (4.6–7.5)	–	2.7 (1.3–4.2)	9.8 (8.2–11.5)
Palinuro	PL	14	5.2 (4.1–6.2)	–	1.7 (1.3–2.2)	9.7 (8.1–11.4)
Scilla	SC	14	6.5 (4.5–8.4)	–	2.1 (1.0–3.2)	12.1 (10.9–13.3)
Pantelleria	PN	14	5.7 (4.3–7.0)	–	1.1 (0.7–1.6)	8.5 (6.2–10.7)

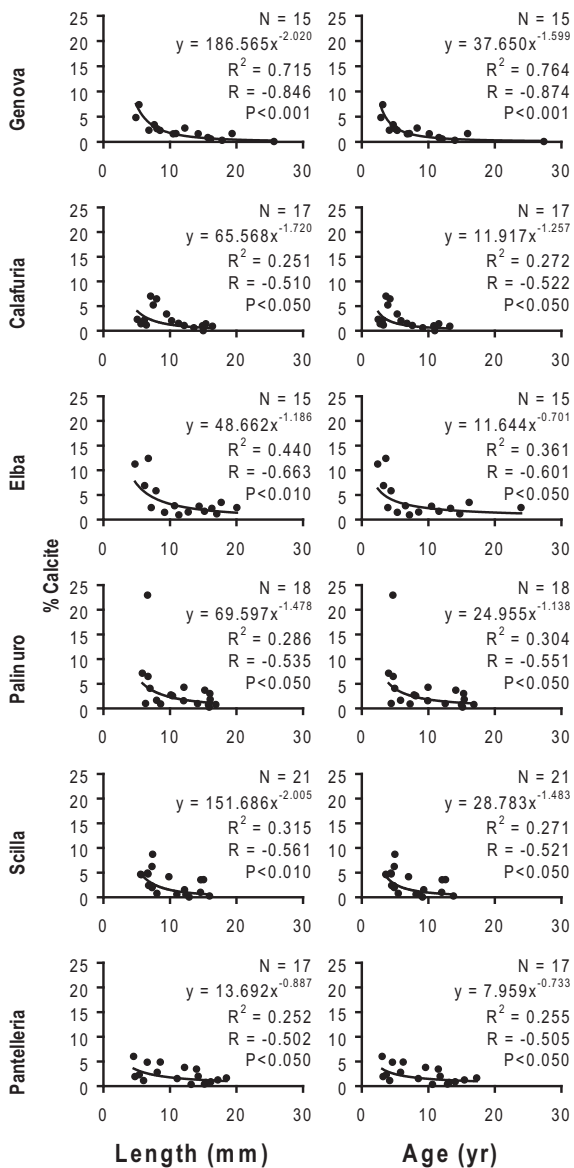


Fig. 5. *Balanophyllia europaea*. Relationships between calcite content, skeleton length and age in the populations. *N*, number of individuals. *R*² and *R*, Pearson's determination and correlation coefficients. The populations are arranged in order of decreasing latitude.

content = 1.9%; Tukey's HSD; Table 1). Calcite content was never correlated with skeleton length (nor age) in any studied site ($P > 0.05$).

3.2. Skeleton section composition

In 64.8% of the sections of *B. europaea* skeletons and in 85.2% of those of *L. pruvoti* calcite was found in addition to aragonite. In all of the population of both species, the highest content of calcite was observed in the aboral sections (Table 2). At four sites out of six (Calafuria, Elba, Scilla and Pantelleria), mean calcite content of the aboral sections of *B. europaea* was significantly higher than that of the oral

ones (Kruskal–Wallis test, $P < 0.05$; Fig. 6). Results on *L. pruvoti* were similar, i.e. in five out of six sites (Genova, Elba, Palinuro, Pantelleria e Calafuria) the calcite content of the aboral sections was significantly higher than the one of the oral sections (Kruskal–Wallis test, $P < 0.05$; Fig. 6). No correlation was observed among magnesium content in the calcite structure and aboral/oral location of the section (Table 3).

Similarly to whole skeletons, calcite content of the sections of *B. europaea* was negatively correlated with the average age of the coral at the time of deposition of the section (Fig. 7). The age of the coral at the time of deposition of the section explained 30.3% of calcite content variance (Fig. 7).

3.3. Skeleton external layer composition

The mineralogy of the external layer of skeletons was studied only by FTIR spectroscopy, since the low amount of collected sample did not allow an X-ray powder diffraction investigation. In all analyzed samples from the basal plate and from the epitheca, calcite was detected along with aragonite (Fig. 3), whereas in the oral region of the skeleton wall, only aragonite was found. The SEM observations and the EDX analyses showed that the epitheca and the basal plate had a different texture and elemental composition than the oral region of skeleton wall and the inner septa. In epitheca and basal plate regions, the mineral texture generated an architectural assembly of the crystal characterized by fenestrated polygons in which magnesium was present (Fig. 3Piii). Instead, the septa had the classical crystalline architecture expected in corals (Fig. 3Pi).

4. DISCUSSION

The significant amount of calcite detected in most of whole skeletons and sections of *B. europaea* and *L. pruvoti* shows that the skeleton of modern corals do not contain pure aragonite like it was generally suggested in the literature in the 1970s (Dodd, 1967; Kinsman, 1969; Livingston and Thompson, 1971; Amiel et al., 1973; Vandermeulen and Watabe, 1973; Weber, 1973, 1974; MacIntyre and Towe, 1976). Although lower than what observed in *Porites* in the 1970s (average calcite 23.8%; Houck et al., 1975), the amount of calcite observed in the present study (1.1–5.8% on average) is similar to what is recently reported for *Porites* (5% on average; Zakaria et al., 2008). The amount of calcite in coral skeletons varied among study sites for *L. pruvoti*, suggesting the effect of local environmental conditions on the type of CaCO_3 composing the skeleton.

Different processes could explain the presence of calcite along the observed axial gradient in *B. europaea* and *L. pruvoti*: (1) a biological control of the coral on the polymorph of calcium carbonate deposited, (2) an introduction of exogenous calcite rich material produced by other organisms, especially crustose coralline algae or borers, and/or (3) diagenetic processes (Fig. 6).

The negative correlation between calcite content and both skeleton length and age in *B. europaea* (Fig. 5), coupled with the observation of a higher calcite content in aboral sections than in oral ones (Fig. 6), could indicate

Table 2

Balanophyllia europaea and *Leptopsammia pruvoti*. Mean calcite content in section samples of the populations. Values in parentheses are the 95% confidence intervals. Number of sections is three per population per section type (aboral, intermediate or oral).

Population	Code	Aboral section	Intermediate section	Oral section
<i>Balanophyllia europaea</i>				
Genova	GN	2.4 (1.0–3.8)	1.4 (0.0–2.9)	0.6 (0.1–1.1)
Calafuria	CL	3.6 (0.0–7.6)	0.6 (0.4–0.7)	0.2 (0.0–0.3)
Elba	LB	9.8 (1.1–18.6)	2.0 (0.6–3.5)	0.6 (0.2–0.9)
Palinuro	PL	3.7 (0.8–6.7)	1.1 (0.0–2.7)	0.6 (0.0–1.3)
Scilla	SC	4.2 (0.9–7.5)	0.2 (0.0–0.5)	0.1 (0.0–0.2)
Pantelleria	PN	3.9 (0.0–8.2)	0.9 (0.5–1.3)	0.2 (0.0–0.4)
<i>Leptopsammia pruvoti</i>				
Genova	GN	3.7 (0.0–7.6)	1.3 (0.9–1.8)	0.5 (0.2–0.7)
Calafuria	CL	6.3 (2.4–10.3)	1.5 (0.6–2.4)	1.2 (0.0–2.7)
Elba	LB	4.2 (3.3–5.0)	1.4 (0.8–2.1)	1.3 (0.0–3.0)
Palinuro	PL	6.1 (0.0–13.5)	1.2 (0.9–1.5)	0.8 (0.0–1.9)
Scilla	SC	3.6 (1.2–6.0)	1.5 (0.3–2.6)	1.7 (0.8–2.5)
Pantelleria	PN	1.9 (0.7–3.2)	2.0 (1.0–3.0)	0.3 (0.2–0.5)

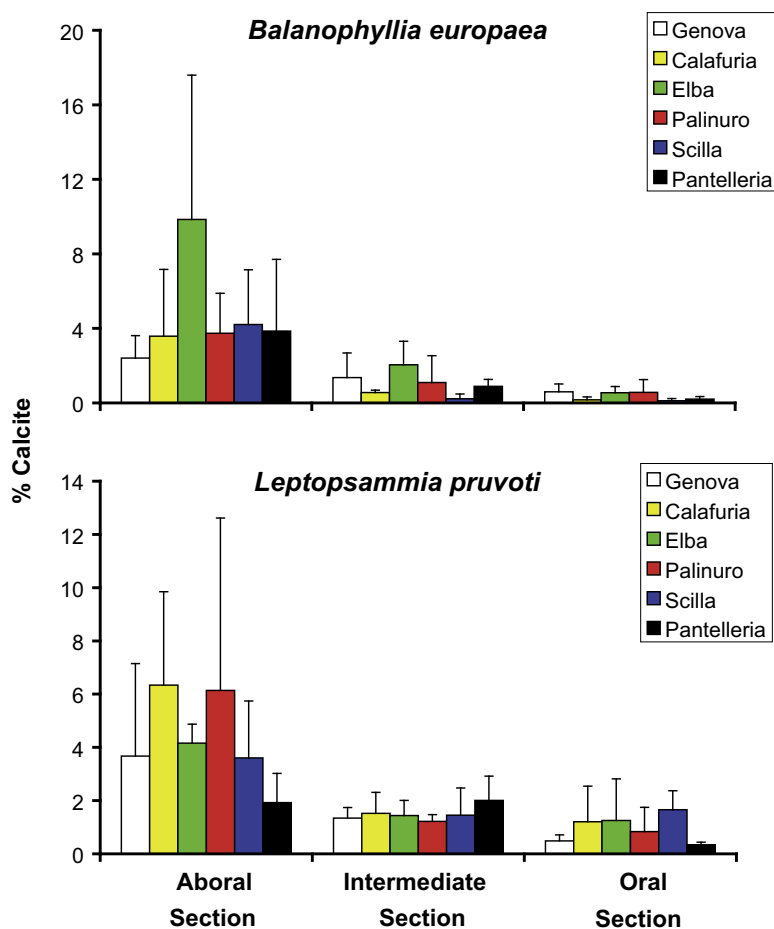


Fig. 6. *Balanophyllia europaea* and *Leptopsammia pruvoti*. Average calcite content of the sections of skeletons in the populations. Error bars represent the standard deviation. Number of corals is three for each population for each species.

that the skeletal elements produced in the first years of growth are significantly more enriched in calcite than those accrued as the polyp gets older. A similar negative correlation between calcite content in the sections and the average

age of the coral at time of the deposition of the section was also found (Fig. 7). This finding is in agreement with a calcite deposit in skeletons of *P. damicornis* during the period following larval settlement (Vandermeulen and Watabe,

Table 3

Balanophyllia europaea and *Leptopsammia pruvoti*. Mean % Mg to Ca substitution in the calcite content of section samples of the populations. Values in parentheses are the 95% confidence intervals. Number of sections is three per population per section type (aboral, intermediate or oral).

Population	Code	Aboral section	Intermediate section	Oral section
<i>Balanophyllia europaea</i>				
Genova	GN	13.3 (10.9–15.7)	6.9 (0.0–14.6)	12.6 (7.1–18.0)
Calafuria	CL	11.5 (5.4–17.5)	8.2 (5.7–10.6)	14.3 (10.9–17.6)
Elba	LB	14.8 (13.7–15.9)	15.5 (14.8–16.1)	8.6 (3.2–14.1)
Palinuro	PL	11.0 (10.5–11.4)	10.4 (10.2–10.5)	4.83 (4.76–4.89)
Scilla	SC	13.0 (10.3–15.6)	7.8 (0.0–16.5)	8.0 (4.2–11.9)
Pantelleria	PN	10.4 (3.1–17.7)	12.3 (9.5–15.1)	10.9 (6.3–15.5)
<i>Leptopsammia pruvoti</i>				
Genova	GN	11.9 (9.6–14.3)	13.5 (8.5–18.4)	12.5 (7.8–17.3)
Calafuria	CL	12.7 (11.2–14.3)	8.7 (7.1–10.4)	12.0 (10.1–13.9)
Elba	LB	10.5 (8.8–12.1)	7.7 (3.6–11.8)	12.8 (8.9–16.7)
Palinuro	PL	12.3 (9.1–15.5)	11.9 (8.7–15.1)	12.1 (11.5–12.6)
Scilla	SC	10.9 (6.3–15.5)	11.7 (7.7–15.6)	9.6 (4.0–15.3)
Pantelleria	PN	15.7 (10.1–21.4)	12.6 (11.9–13.2)	7.2 (3.2–11.1)

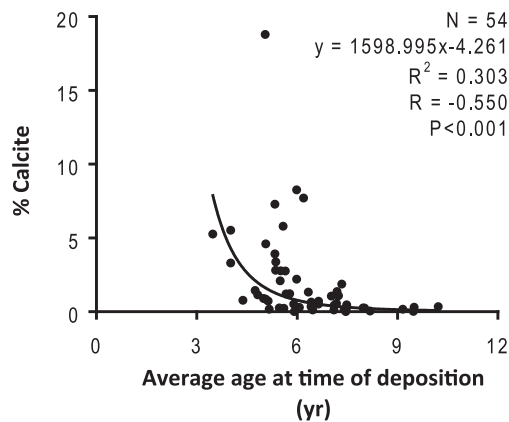


Fig. 7. *Balanophyllia europaea*. Dependence of calcite content on average age of the coral at time of deposition of the section. N , number of individuals. R^2 and R , Pearson's determination and correlation coefficients.

1973). However, a recent analysis of the mineralogy of newly settled (10 days) *Acropora millepora* recruits have not revealed phases other than aragonite, within the detection limits of the techniques used (minimum detectable amount = 5%; Clode et al., 2010). The presence of calcite in addition to aragonite in the post settlement phase and at the base of the skeleton could confer an adaptive advantage to this species. Calcite could act as cement that favours the anchoring of the coral to the substrate, in a similar fashion to the consolidating action of crustose coralline red algae (Littler and Littler, 1988), and could protect the exposed septa in the aboral region. This skeletal feature could confer to *B. europaea* a better chance of remaining attached to the substrate in the high wave energy and strong current environment, typical of the shallow waters it colonizes (Zibrowius, 1980). Moreover, the plate region in *B. europaea* shows macroscopic scale smoothness (Fig. 3a, Vb) that could facilitate the adhesion of the coral to the substrate by increasing the skeleton-substrate surface

contact area. Recent *in vitro* studies show that intracrystalline macromolecules extracted from the skeleton of *B. europaea* are able to affect the *in vitro* calcium carbonate deposition, favouring under particular conditions (i.e. water soluble/insoluble protein ratios) the precipitation of specific polymorphs of calcium carbonate even when the artificial environmental conditions would favour other polymorphs (Goffredo et al., 2011). *L. pruvoti*, instead, living in deeper waters and inside caves and overhangs (Zibrowius, 1980), is subjected to lower hydrodynamic stress and would not need to concentrate calcite in the first years of growth (Burton and Walter, 1997). This could explain the lack of correlations between *L. pruvoti* length (age) and calcite content. Further analyses are necessary to clarify this relationship and must combine analysis of skeletons from different coral species living under different environmental conditions (water chemistry and physics).

The origin of calcite in aboral sections could also result from a "pollution" due to the growth of other calcifying organisms. This observation is supported by the different mineral texture observed in the external layer of the basal plate and of the epitheca (Fig 3). On Fig 3A Piii, the structure observed is obviously that of a crustose coralline algae (CCA) (see SEM images of CCA reported in Ries, 2006). CCA are known to be one of the most suitable substrates for coral settlement in tropical environments (Morse et al., 1988; Heyward and Negri, 1999; Raimondi and Morse, 2000; Baird and Morse, 2004; Harrington et al., 2004; Golbuu and Richmond, 2007). Recently, significant amounts of calcite have been found in the epitheca and basal plate of *Balanophyllia regia* encrusted by CCA (Brahmi et al., 2010). CCA are likely to be one of the sources of calcite found in our samples. EDS analyses showed that the content of magnesium is clearly detectable in the calcite produced by these encrusting organisms (Fig. 8). In the coral produced calcium carbonate, no magnesium was detectable, while strontium amounts were always found, indicating the presence of aragonite (Fig. 8). In some of our samples, calcite may also come from serpulid tubes.

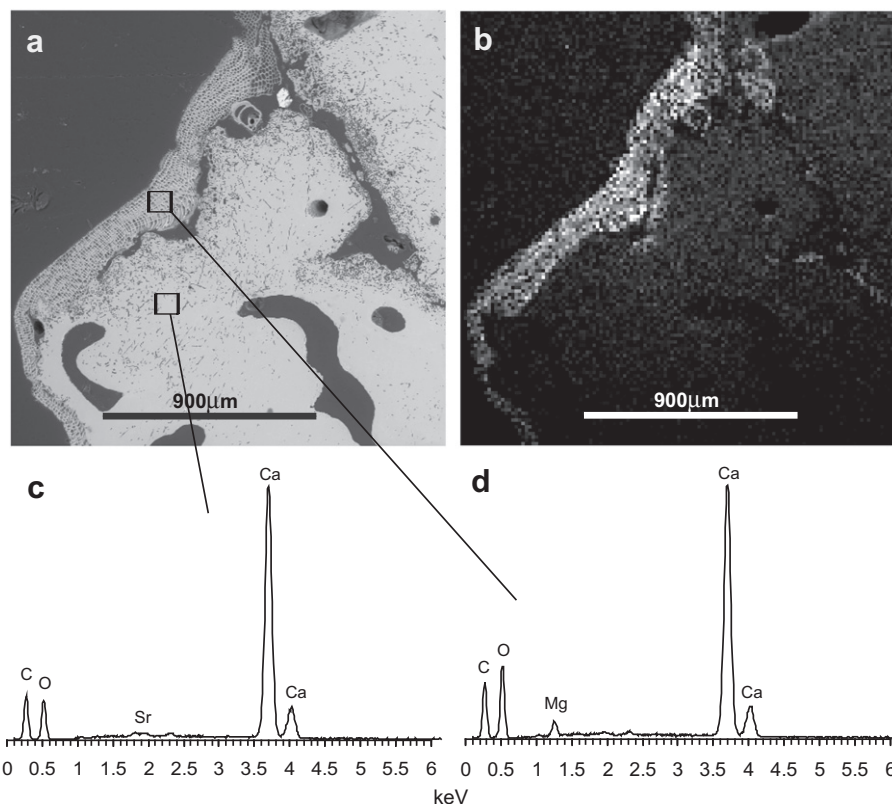


Fig. 8. *Balanophyllia europaea*. (a) Section of a skeleton encrusted by CCAs. (b) Corresponding EDS map for Magnesium distribution. Whiter spots contain a higher content of Magnesium, and are located in the material produced by CCAs. (c) EDS spectrum of the coral produced (endogenous) calcium carbonate. Strontium is detected while no Magnesium peak is visible. (d) EDS spectrum of the CCA produced (exogenous) calcium carbonate. Magnesium is detected while no Strontium peak is visible.

XRD analyses of powder obtained by grinding serpulid tubes confirmed that they are mainly composed of calcite (Neff, 1971). Some scleractinian larvae may preferentially settle on this type of substrate (Golbuu and Richmond, 2007). In such a case, the skeletal material produced by the coral could be so closely associated with the calcitic tube that our procedure of removal of exogenous material may have been ineffective. However, even the oral sections of both species, where no serpulid tubes were ever seen during sample preparation, showed significant content of calcite. Presence of calcite in the oral region of coral skeletons cannot therefore be explained by the hypothesis of a “pollution” of coral skeletons by exogenous calcite precipitated by serpulids or other calcifiers.

In the oral region of corals, calcite may come from filling of microborings although no boreholes were observed in the present study. These microorganisms are known to be present in both dead and alive carbonate substrates such as the massive scleractinian coral, *Porites lobata* (Le Campion-Alsumard et al., 1995; Tribollet, 2008) and the crustose coralline alga *Hydrolithon onkodes* (Tribollet and Payri, 2001). Microborers comprise phototrophic and heterotrophic organisms including cyanobacteria, microalgae and fungi (see the review by Tribollet (2008)). Primary production by microborers and other microorganisms present inside dead coral skeletons is important (Tribollet et al.,

2006), thus modifying the intra-skeleton environment in terms of pH (Risk and Kramer, 1981), oxygen and nutrient concentrations (Bellamy and Risk, 1982; Risk and Muller, 1983; Ferrer and Szmant, 1988). In live corals, only few microboring species are able to keep up with coral growth and form in general a green or black band beneath the layer of coral tissues (Le Campion-Alsumard et al., 1995; Priess et al., 2000). Microborers are less abundant in live coral skeletons than in dead ones, and due to the limited amount of light reaching them, their photosynthetic activity is reduced (Kanwisher and Wainwright, 1967; Fork and Larkum, 1989; Magnusson et al., 2007). However, in some live colonies of *Porites lobata*, boreholes of filamentous microborers are abundant, located close to the coral surface, and up to 20% of them can be filled with calcite (Nothdurft et al., 2007). Nothdurft et al. (2007) could not highlight the process involved in calcite precipitation in microborings, but suggested that it might be due to microborer metabolic activity. In dead carbonate substrates such as sand grains, Kobluk and Risk, (1977) showed that microborers are involved in micritisation in coral reefs. On one end of microboring filaments (deep inside carbonate substrates), dissolution occurs probably because of the presence of Ca^{2+} pumps (see review of mechanisms involved in dissolution of carbonates by microborers in Tribollet, 2008; Garcia-Pichel et al., 2010) and on the other

end (area of the filaments in contact with seawater), the released calcium precipitates with carbon to produce CaCO_3 such as Mg-calcite (Schroeder, 1972; Garcia-Pichel et al., 2010) under specific environmental conditions. In the present study, the fact that the overall calcite content in skeletons (1–6%; Table 1) grown in situ (Mg/Ca about 5; de Villiers and Nelson, 1999) is considerably lower than the one observed in corals grown in artificial seawater with Mg/Ca ratio of 3.5 (calcite = 10–12%; Ries et al., 2006) suggests that the relatively high-Mg calcite incorporated into the Mediterranean coral skeleton is derived from a high-Mg calcitic organism that has encrusted the skeleton (such as CCAs), or from the averaging of low and high-Mg calcitic depositions. Yet another hypothetical source of calcite contamination could be a non-biological surface-induced precipitation (or overgrowth) of magnesium calcite on the basal plate and the epitheca, associated with the peculiar chemistry that may take place at the aragonite–seawater interface (Falini et al., 2005; Falini et al., 2009). Finally it could also result from diagenesis which occurs in coral skeletons, including those of live organisms.

In any case, the amount of CaCO_3 precipitated inside coral skeletons other than aragonite can potentially affect the analysis of coral archives in paleoclimatic studies (based on Sr/Ca or Mg/Ca ratios, or oxygen stable isotopes), which requires pure aragonitic substrates (Allison, 1996; Nothdurft et al., 2007). Cements present in microborings or resulting from early diagenetic processes grow in micro-environments where the water chemistry do not reflect the one of ambient seawater, with important implications for paleoclimatic archives (Muller et al., 2001; Nothdurft and Webb, 2009b). Boring-filling calcite inclusions may have very different ion concentrations than the coral-produced skeletal material (Allison, 1996; Nothdurft et al., 2007). In *Porites*, it is estimated that the inclusion of only 1% of microborer-derived calcite in an aragonitic coral sample used for paleothermometry can bias the calculated temperature (derived by the Sr/Ca ratio) of 0.5–1.2 °C (Allison et al., 2007; Nothdurft et al., 2007; Dalbeck et al., 2011). In the case of Mg/Ca temperature reconstruction, it is estimated that the inclusion of 1% of calcite cement in the aragonitic coral skeleton will increase the estimated temperature of 4–11 °C (Allison et al., 2007). The origin of calcite and its implications inside coral skeletons should be therefore further investigated if paleoclimate and paleo-environments have to be precisely and accurately reconstructed. Previous studies reported the presence of calcite-filled borings in 20% of the analyzed *Porites* samples, where they can occupy up to 60% of total skeletal volume, and suggested that samples used for paleoclimatic reconstruction be inspected using SEM after a polish-etching to avoid using samples particularly affected by microborers (Nothdurft et al., 2007; Nothdurft and Webb, 2009b). In the present study, calcite was found in more than 90% of the analyzed samples, suggesting that some coral species may be particularly subjected to boring and may be more contaminated by exogenous sources of calcium carbonate. Thus, the suggestion of a preliminary inspection by SEM after polish-etching before the paleoclimatic analyses is strongly emphasized.

ACKNOWLEDGEMENTS

This study is part of the FP7 IDEAS EU-Research Project “CoralWarm” (Grant Agreement no. 249930). We thank L. Bortolazzi, A. Comini, M. Cova, G. Gasparini, P. Bonzi, M. Ghelia, G. Neto, and L. Tomesani for their underwater assistance in collecting the samples. The diving centres Centro Immersioni Pantelleria, Il Pesciolino, Polo Sub, and Sub Maldive supplied logistic assistance in the field. The Bologna Scuba Team (BST) and the Scientific Diving School (SDS) collaborated in the underwater activities. The Marine Science Group (<http://www.marine-sciencegroup.org>) supplied scientific, technical, and logistical support. This research was financed by the Ministry of Education, University and Research (MIUR), the Ministry of Tourism of the Arab Republic of Egypt, the Associazione dei Tour Operator Italiani (ASTOI), the Project AWARE Foundation, the Scuba Nitrox Safety International (SNSI), the Scuba Schools International (SSI), the Underwater Life Project (ULP), the Marine & Freshwater Science Group Association, and the Consorzio Interuniversitario di Ricerca della Chimica dei Metalli nei Sistemi Biologici. The experiments complied with current Italian law.

APPENDIX A. SUPPLEMENTARY DATA

Supplementary data associated with this article can be found, in the online version, at <http://dx.doi.org/10.1016/j.gca.2012.02.014>.

REFERENCES

- Allison N. (1996) Geochemical anomalies in coral skeletons and their possible implications for paleoenvironmental analyses. *Mar. Chem.* **55**, 367–379.
- Allison N., Finch A. A., Webster J. M. and Clague D. A. (2007) Palaeoenvironmental records from fossil corals: the effects of submarine diagenesis on temperature and climate estimates. *Geochim. Cosmochim. Acta* **71**, 4693–4703.
- Altomare A., Burla M. C., Giacomazzo C., Guagliardi A., Moliterni A. G. G., Polidori G. and Rizzi R. (2001) Quanto: a Rietveld program for quantitative phase analysis of polycrystalline mixtures. *J. Appl. Cryst.* **34**, 392–397.
- Amiel A. J., Friedman G. M. and Miller D. S. (1973) Distribution and nature of incorporation of trace elements in modern aragonite corals. *Sedimentology* **20**, 47–64.
- Baird A. H. and Morse A. N. C. (2004) Induction of metamorphosis in larvae of the brooding corals *Acropora palifera* and *Stylophora pistillata*. *Mar. Freshw. Res.* **55**, 469–472.
- Bellamy N. and Risk M. J. (1982) Coral gas: oxygen production in *Millepora* on the Great Barrier Reef. *Science* **215**, 1618–1619.
- Brahmi C., Meibom A., Smith D. C., Stolarski J., Auzoux-Bordenave S., Nouet J., Doumenc D., Djediat C. and Domart-Coulon I. (2010) Skeletal growth, ultrastructure and composition of the azooxanthellate scleractinian coral *Balanophyllia regia*. *Coral Reefs* **29**, 175–189.
- Burton E. M. and Walter L. M. (1997) Relative precipitation rates of aragonite and Mg calcite from seawater: temperature or carbonate ion control? *Geology* **15**, 111–114.
- Chadwick-Fuman N. E., Goffredo S. and Loya Y. (2000) Growth and population dynamic model of the reef coral *Fungia granulosa* Kluzinger, 1879 at Eilat, northern Red Sea. *J. Exp. Mar. Biol. Ecol.* **249**, 199–218.
- Clode P. L., Lema K., Saunders M. and Weiner S. (2010) Skeletal mineralogy of newly settling *Acropora millepora* (Scleractinia) coral recruits. *Coral Reefs* **30**, 1–8.

- Cuif J. P. and Dauphin Y. (2005) The environment recording unit in coral skeletons – a synthesis of structural and chemical evidences for a biochemically driven, stepping-growth process in fibres. *Biogeosciences* **2**, 61–73.
- Dalbeck P., Cusack M., Dobson P. S., Allison N., Fallick A. E., Tudhope A. W. and EIMF (2011) Identification and composition of secondary meniscus calcite in fossil coral and the effect on predicted sea surface temperature. *Chem. Geol.* **280**, 314–322.
- De Villiers S. and Nelson B. K. (1999) Detection of low-temperature hydrothermal fluxes by seawater Mg and Ca anomalies. *Science* **285**, 721–723.
- Dodd J. R. (1967) Magnesium and strontium in calcareous skeletons; a review. *J. Paleontol.* **41**, 1313–1329.
- Falini G., Gazzano M. and Ripamonti A. (1994) Crystallization of calcium carbonate in presence of magnesium and polyelectrolytes. *J. Cryst. Growth* **137**, 577–584.
- Falini G., Fermani S., Maritic M., Vanzo S. and Zaffino G. (2005) Influence on aragonite or vaterite formation by otolith macromolecules. *Eur. J. Inorg. Chem.* **1**, 162–167.
- Falini G., Fermani S., Tosi G. and Dinelli E. (2009) Calcium carbonate morphology and structure in the presence of sea water ions and humic acids. *Cryst. Growth Des.* **9**, 2065–2072.
- Ferrer L. M. and Szmat A. M. (1988) Nutrient regeneration by the endolithic communities in coral skeletons. *Proc. 6th Int. Coral Reef Symp., Townsville* **3**, 1–4.
- Fork D. C. and Larkum A. D. W. (1989) Light harvesting in the green alga *Ostreobium sp.*, a coral symbiont adapted to extreme shade. *Mar. Biol.* **103**, 381–385.
- Garcia-Pichel F., Ramírez-Reinat E. and Gao Q. (2010) Microbial excavation of solid carbonates powered by P-type ATPase-mediated transcellular Ca^{2+} transport. *Proc. Natl. Acad. Sci. USA*. <http://dx.doi.org/10.1073/pnas.1011884108>.
- Goffredo S. and Chadwick-Furman N. E. (2003) Comparative demography of mushroom corals (Scleractinia, Fungiidae) at Eilat, northern Red Sea. *Mar. Biol.* **142**, 411–418.
- Goffredo S., Arnone S. and Zaccanti F. (2002) Sexual reproduction in the Mediterranean solitary coral *Balanophyllia europaea* (Scleractinia, Dendrophylliidae). *Mar. Ecol. Prog. Ser.* **229**, 83–94.
- Goffredo S., Mattioli G. and Zaccanti F. (2004a) Growth and population dynamics model of the Mediterranean solitary coral *Balanophyllia europaea* (Scleractinia, Dendrophylliidae). *Coral Reefs* **23**, 433–443.
- Goffredo S., Mezzomonaco L. and Zaccanti F. (2004b) Genetic differentiation among populations of the Mediterranean hermaphroditic brooding coral *Balanophyllia europaea* (Scleractinia, Dendrophylliidae). *Mar. Biol.* **145**, 1075–1083.
- Goffredo S., Airi V., Radetić J. and Zaccanti F. (2006) Sexual reproduction of the solitary sunset cup coral *Leptopsammia pruvoti* (Scleractinia, Dendrophylliidae) in the Mediterranean. 2. Quantitative aspects of the annual reproductive cycle. *Mar. Biol.* **148**, 923–932.
- Goffredo S., Caroselli E., Pignotti E., Mattioli G. and Zaccanti F. (2007) Variation in biometry and population density of solitary corals with solar radiation and sea surface temperature in the Mediterranean Sea. *Mar. Biol.* **152**, 351–361.
- Goffredo S., Caroselli E., Mattioli G., Pignotti E. and Zaccanti F. (2008) Relationships between growth, population structure and sea surface temperature in the temperate solitary coral *Balanophyllia europaea* (Scleractinia, Dendrophylliidae). *Coral Reefs* **27**, 623–632.
- Goffredo S., Caroselli E., Mattioli G., Pignotti E., Dubinsky Z. and Zaccanti F. (2009a) Inferred level of calcification decreases along an increasing temperature gradient in a Mediterranean endemic coral. *Limnol. Oceanogr.* **54**, 930–937.
- Goffredo S., Di Ceglie S. and Zaccanti F. (2009b) Genetic differentiation of the temperate-subtropical stony coral *Leptopsammia pruvoti* in the Mediterranean Sea. *Israel J. Ecol. Evol.* **55**, 99–115.
- Goffredo S., Vergni P., Reggi M., Caroselli E., Sparla F., Levy O., Dubinsky Z. and Falini G. (2011) The skeletal organic matrix from Mediterranean coral *Balanophyllia europaea* influences calcium carbonate precipitation. *PLoS ONE* **6**, e22338.
- Golbuu Y. and Richmond R. (2007) Substratum preferences in planula larvae of two species of scleractinian corals, *Goniastrea retiformis* and *Stylaraea punctata*. *Mar. Biol.* **152**, 639–644.
- Goldsmith J. R., Graf D. L. and Heard H. C. (1961) Lattice constants of calcium–magnesium carbonates. *Am. Mineral.* **46**, 453–457.
- Harrington L., Fabricius K., De'ath G. and Negri A. (2004) Recognition and selection of settlement substrata determine post-settlement survival in corals. *Ecology* **85**, 3428–3437.
- Heyward A. J. and Negri A. P. (1999) Natural inducers for coral larval metamorphosis. *Coral Reefs* **18**, 273–279.
- Houck J. E., Buddemeier R. W. and Chave K. E. (1975) Skeletal low-magnesium calcite in living scleractinian corals. *Science* **189**, 997–999.
- Kanwisher J. W. and Wainwright S. A. (1967) Oxygen balance in some reef corals. *Biol. Bull.* **133**, 378–390.
- Kinsman D. J. J. (1969) Interpretation of Sr+2 concentration in carbonate minerals and rocks. *J. Sediment. Res.* **39**, 486–508.
- Le Campion-Alsumard T., Golubic S. and Hutchings P. (1995) Microbial endoliths in skeletons of live and dead corals: *Porites lobata* (Moorea, French Polynesia). *Mar. Ecol. Prog. Ser.* **117**, 149–157.
- Littler M. M. and Littler D. S. (1988) Structure and role of algae in tropical reef communities. In *Algae and Human Affairs* (eds. C. A. Lembi and J. R. Waaland). Cambridge University Press, Cambridge, pp. 29–56.
- Livingston H. D. and Thompson G. (1971) Trace element concentrations in some modern corals. *Limnol. Oceanogr.* **16**, 786–796.
- MacIntyre I. G. and Towe K. M. (1976) Skeletal calcite in living scleractinian corals: microboring fillings, not primary skeletal deposits. *Science* **193**, 701–702.
- Magnusson S. H., Fine M. and Kühl M. (2007) Light microclimate of endolithic phototrophs in the scleractinian corals *Montipora monasteriata* and *Porites cylindrica*. *Mar. Ecol. Prog. Ser.* **332**, 119–128.
- Marchegiani F., Cibej E., Vergni P., Tosi G., Fermani S. and Falini G. (2009) Hydroxyapatite synthesis from biogenic calcite single crystals into phosphate solutions at ambient conditions. *J. Cryst. Growth* **311**, 4219–4225.
- Morse D. E., Hooker N., Morse A. N. C. and Jensen R. A. (1988) Control of larval metamorphosis and recruitment in sympatric agariciid corals. *J. Exp. Mar. Biol. Ecol.* **116**, 193–217.
- Muller A., Gagan M. K. and McCulloch M. T. (2001). *Geophys. Res. Lett.* **28**, 4471–4474.
- Mundet L. and Ribera L. (2001) Characteristics of divers at Spanish resort. *Tourism Manage.* **22**, 201–510.
- Neff J. M. (1971) Ultrastructural studies of the secretion of calcium carbonate by the serpulid polychaete worm, *Pomatoceros caeruleus*. *Zeitschrift fuer Zellforschung und Mikroskopische Anatomie* **120**, 160–186.
- Nothdurft L. D. and Webb G. E. (2009a) Clypeotheca, a new skeletal structure in scleractinian corals: a potential stress indicator. *Coral Reefs* **28**, 143–153.
- Nothdurft L. D. and Webb G. E. (2009b) Earliest diagenesis in scleractinian coral skeletons: implications for paleoclimate-sensitive geochemical archives. *Facies* **55**, 161–201.

- Nothdurft L. D., Webb G. E., Bostrom T. and Rintoul L. (2007) Calcite-filled borings in the most recently deposited skeleton in live-collected *Porites* (Scleractinia): implications for trace element archives. *Geochim. Cosmochim. Acta* **71**, 5423–5438.
- Pingitore N. E., Fretzdorf S. B., Seitz B., Estrada L., Borrego P., Crawford G. and Love K. (1993) Dissolution kinetics of CaCO₃ in common laboratory solvents. *J. Sed. Petrol.* **63**, 641–645.
- Potvin C. and Roff D. A. (1993) Distribution-free and robust statistical methods: viable alternatives to parametric statistics? *Ecology* **74**, 1617–1628.
- Priess K., Le Campion-Alsumard T., Golubic S., Gadel F. and Thomassin B. A. (2000) Fungi in corals: black bands and density-banding of *Porites lutea* and *P. lobata* skeleton. *Mar. Biol.* **136**, 19–27.
- Raimondi P. T. and Morse A. N. C. (2000) The consequences of complex larval behavior in a coral. *Ecology* **81**, 3193–3211.
- Ries J. B. (2006) Mg fractionation in crustose coralline algae: geochemical, biological, and sedimentological implications of secular variation in the Mg/Ca ratio of seawater. *Geochim. Cosmochim. Acta* **70**, 891–900.
- Ries J. B., Stanley S. M. and Hardie L. A. (2006) Scleractinian corals produce calcite, and grow more slowly, in artificial Cretaceous seawater. *Geology* **34**, 525–528.
- Risk M. J. and Kramer J. R. (1981) Water chemistry inside coral heads: determination of pH, Ca and Mg. *Proc. 4th Int. Coral Reef Symp. Manila*, **1**, 54.
- Risk M. J. and Muller H. R. (1983) Porewater in coral heads: evidence for nutrient regeneration. *Limnol. Oceanogr.* **28**, 1004–1008.
- Schroeder J. H. (1972) Calcified filaments of an endolithic alga in recent Bermuda reefs. *Neues Jahrb. Geol. Paläontol. Monatsh.* **1**, 16–33.
- Scott P. J. B. and Risk M. J. (1988) The effect of *Lithophaga* (Bivalvia: Mytilidae) boreholes on the strength of the coral *Porites lobata*. *Coral Reefs* **7**, 145–151.
- Tribollet A. (2008) The boring microflora in modern coral reefs: a review of its roles. In *Current Developments in Bioerosion* (eds. M. Wisshak and L. Tapanila). Springer-Verlag, Berlin-Heidelberg, pp. 67–94.
- Tribollet A. and Payri C. (2001) Bioerosion of the crustose coralline alga *Hydrolithon onkodes* by microborers in the coral reefs of Moorea, French Polynesia. *Oceanolog. Acta* **24**, 329–342.
- Tribollet A. and Golubic S. (2011) Reef bioerosion: agents and processes. In *Coral Reefs: An Ecosystem in Transition* (eds. Z. Dubisnky and N. Stambler). Springer, Dordrecht–Heidelberg–London–New York, pp. 435–449.
- Tribollet A., Langdon C., Golubic S. and Atkinson M. (2006) Endolithic microflora are major primary producers in dead carbonate substrates of Hawaiian coral reefs. *J. Phycol.* **42**, 292–303.
- Tukey J. W. (1949) Comparing individual means in the analysis of variance. *Biometrics* **5**, 99–114.
- Vandermeulen J. H. and Watabe N. (1973) Studies on reef corals. I. Skeleton formation by newly settled planula of *Pocillopora damicornis*. *Mar. Biol.* **23**, 47–57.
- Vongsavat V., Winotai P. and Meejoo S. (2006) Phase transitions of natural corals monitored by ESR spectroscopy. *Nucl. Instr. Meth. B* **243**, 167–173.
- Weber J. N. (1973) Incorporation of strontium into reef coral skeletal carbonate. *Geochim. Cosmochim. Acta* **37**, 2173–2190.
- Weber J. N. (1974) Skeletal chemistry of scleractinian reef corals; uptake of magnesium from seawater. *Am. J. Sci.* **274**, 84–93.
- Zakaria F. Z., Mihály J., Sajó I., Katona R., Hajba L., Aziz F. A. and Mink J. (2008) FT-Raman and FTIR spectroscopic characterization of biogenic carbonates from *Philippine venus* seashell and *Porites* sp. coral. *J. Raman Spectrosc.* **39**, 1204–1209.
- Zibrowius H. (1980) Les scléactiniaires de la Méditerranée et de l'Atlantique nord-oriental. *Mem. Inst. Oceanogr. (Monaco)* **11**, 1–284.

Associate editor: Timothy W. Lyons